

## Prediction of Dynamic Characteristics of Foil Thrust Bearings Using Computational Fluid Dynamics

K. Qin<sup>1</sup>, I. H. Jahn<sup>2</sup> and P. A. Jacobs<sup>1</sup>

<sup>1</sup>Queensland Geothermal Energy Centre of Excellence  
Department of Mechanical and Mining Engineering  
The University of Queensland, Brisbane, Queensland 4072, Australia

<sup>2</sup>Centre for Hypersonics  
Department of Mechanical and Mining Engineering  
The University of Queensland, Brisbane, Queensland 4072, Australia

### Abstract

A three dimensional computational fluid dynamic (CFD) method is proposed to predict rotordynamic coefficients for foil thrust bearings. Unsteady CFD coupled with a two-dimensional structural model is used to solve the transient load capacity of the bearing for the synchronous rotor whirling modes. The rotordynamic coefficient are identified using these transient load capacities and rotor motions. The numerical results show that the rotordynamic coefficients predicted with the proposed method agree well with results in the literature. The proposed method and rotor whirling model can be used to perform a reasonably accurate prediction of the synchronous rotordynamic force coefficients and is able to calculate rotordynamic coefficients of foil thrust bearings across a wide frequency range within a single simulation. Finally, the stiffness and damping coefficients for CO<sub>2</sub> foil thrust bearings are obtained. It is found that CO<sub>2</sub> foil thrust bearings show a smaller damping effect compared to air foil bearings, but the stiffness coefficient is comparable.

### Introduction

Foil bearings are considered a key component to enable high speed turbomachinery system for air-cycle machines [1] and supercritical CO<sub>2</sub> cycles [2]. As foil bearings can use the process fluid as the lubricant, they result in an oil-free turbomachinery system capable of high speed operation. Foil bearings can also provide a longer life, which is critical for the high-speed turbomachinery system. They have been experimentally tested as part of next-generation supercritical CO<sub>2</sub> power cycles development at Sandia National Laboratories [2].

The performance of foil bearings is determined by load capacity, power loss and rotordynamic coefficients. Reynolds equation is widely used to explore the load capacity and power loss of foil thrust bearings. However, it has been shown that Reynolds equation is not adequate for CO<sub>2</sub> foil thrust bearings [3, 4]. CFD can perform a more comprehensive analysis of the fluid behaviours within foil thrust bearings, therefore, it was used to predict the steady state performance of CO<sub>2</sub> foil thrust bearings [3].

CFD can also be expanded to determine the dynamic performance, and it has been widely used to predict the dynamic characteristics of fluid riding seals [5]. Due to the complex geometry of seals, it is hard to predict the dynamic performance of seals using Reynolds equation. There are only a few papers about the determination of dynamic characteristics of foil bearings using CFD. Papadopoulos et. al. [6] determined the stiffness and damping for textured section pad thrust bearings with CFD. For the dynamic performance prediction of bearings, the common approach is to use the small perturbation method [7]. In

this method the steady state position of the rotor is perturbed by small translational and rotational displacements. This paper implements a method to determine stiffness and damping coefficients using CFD and investigates the dynamic characteristics of CO<sub>2</sub> foil thrust bearings.

The paper is organised as follows: firstly, the computational tool for the fluid-structure interaction is briefly introduced. The method to determine the stiffness and damping coefficients from CFD results is then outlined and verified with the results from the literature [1]. Lastly, the dynamic characteristics of CO<sub>2</sub> foil thrust bearings are determined and compared with air foil bearings.

### Computational Model

A computational tool has been developed and validated to simulate foil thrust bearings [3]. This tool consists of a fluid solver and a structural deformation solver. The in-house CFD code Eilmer [8, 9] has been extended for the fluid flow within the foil thrust bearings [3, 10]. The two-dimensional thin plate theory is applied for the deformation of the top foil, while the bump foils are modelled as a spring-like structure [11, 3]. A coupling algorithm is used to map the pressure and deflection between these two solvers [12]. The suitability of this computational tool for foil thrust bearings was demonstrated previously [3]. For the gas model, a look-up table generated with NIST REFPROP [13] is used. For CO<sub>2</sub> this table is based on equation of state by Span and Wagner [14].

### Determination of Rotordynamic Coefficients

The conventional rotordynamic model to quantify reaction forces, for small axial rotor motions is presented in Eqn. 1 [15]. Here all coefficients are assumed frequency dependent and added mass effects are neglected.

$$-f_z(t) = K(\Omega)\Delta z(t) + C(\Omega)\Delta \dot{z}(t), \quad (1)$$

where  $K$  is the stiffness coefficient,  $C$  is the damping coefficient,  $\Omega$  is the excitation frequency,  $f_z$  is the reaction force and  $\Delta z$  is the perturbed rotor position. To find the stiffness and damping coefficients, the transient perturbation method based on the unsteady CFD simulation of a foil thrust bearing is utilised. During the simulation, the rotor surface boundary is perturbed in a periodic motion leading to a corresponding change of the fluid domain. The reaction forces  $f_z$  acting on the rotor due to the rotor motion are obtained by integrating the pressure.

$$f_z(t) = \int (p - p_a) dA_i, \quad (2)$$

where  $p$  is the pressure acting on the rotor surface, while  $p_a$  is

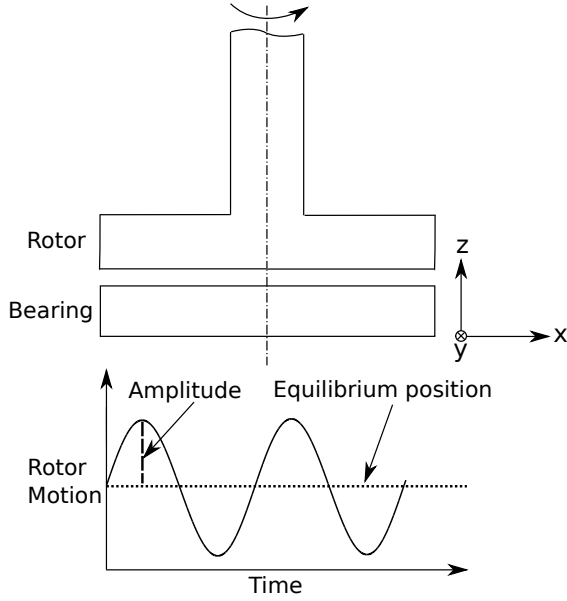


Figure 1: Schematic diagram of rotor perturbation motion.

the ambient pressure, and  $A_i$  is the cell area. The reaction forces have the same frequency as the prescribed rotor movement but are shifted in phase. The rotor position is perturbed using a uni-directional harmonic function.

$$\Delta z(t) = \delta \sin(\Omega t), \quad (3)$$

where the amplitude  $\delta$  is defined as a fraction of the clearance between rotor and bearing and the excitation frequency  $\Omega$  is chosen as a fraction of the rotational speed of the rotor. In this study the fixed amplitude  $\delta$  is fixed to 10% of the clearance, the selection of the perturbation amplitude is investigated in Fig. 5(b). The uni-directional axial perturbation normal to the rotation axis is depicted in Fig. 1, where the clearance between rotor and bearing are exaggerated for visualisation purpose. The rotordynamic coefficients can be determined by analysing the reaction forces due to the prescribed rotor motion. To solve the frequency-dependent rotordynamic coefficients in Eqn. 1, the Laplace transform is performed over the interval  $[0, T]$  and written as

$$F(s) = D(s)Z(s), \quad (4)$$

The time-dependent component are

$$F(s) = \int_0^T f(t)e^{st+\phi} dt \quad (5)$$

$$D(s) = K(\Omega) + sC(\Omega) \quad (6)$$

$$Z(s) = \int_0^T \Delta z(t)e^{st} dt, \quad (7)$$

where  $s = i\Omega$ ,  $i = \sqrt{-1}$  and  $\phi$  is the phase lag between the rotor motion and the reaction forces. The phase lag  $\phi$  between the rotor position and the reaction force is obtained by measuring the peak-to-peak time delay  $\Delta T$  between the harmonic position and force data from the unsteady CFD simulations. This can then be turned into a phase lag using  $\phi = 2\pi\Omega\Delta T$ . As all the component are complex variables,  $F(s)$  and  $Z(s)$  are written as.

$$F(s) = F_r(\Omega) + iF_i(\Omega) \quad (8)$$

$$Z(s) = Z_r(\Omega) + iZ_i(\Omega), \quad (9)$$

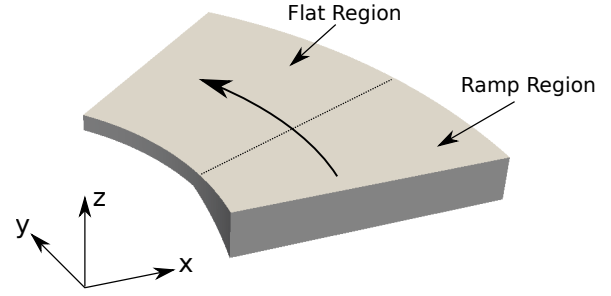


Figure 2: Computational domain for foil thrust bearings, not to scale [3].

The real and imaginary parts of reaction force and rotor motion are computed as [16]

$$Z_r(\Omega) = \frac{1}{2} \sum_{i=1}^n \Delta t [\Delta z(t_i) \cos(\Omega t_i) + \Delta z(t_{i-1}) \cos(\Omega t_{i-1})] \quad (10)$$

$$Z_i(\Omega) = \frac{1}{2} \sum_{i=1}^n \Delta t [\Delta z(t_i) \sin(\Omega t_i) + \Delta z(t_{i-1}) \sin(\Omega t_{i-1})] \quad (11)$$

$$F_r(\Omega) = \frac{1}{2} \sum_{i=1}^n \Delta t [f(t_i) \cos(\Omega t_i) + f(t_{i-1}) \cos(\Omega t_{i-1})] \quad (12)$$

$$F_i(\Omega) = \frac{1}{2} \sum_{i=1}^n \Delta t [f(t_i) \sin(\Omega t_i) + f(t_{i-1}) \sin(\Omega t_{i-1})], \quad (13)$$

By substituting Eqns. 6, 8 and 9 into Eqn. 4, the following equations are obtained

$$F_r = K(\Omega)Z_r - \Omega C(\Omega)Z_i \quad (14)$$

$$F_i = K(\Omega)Z_i + \Omega C(\Omega)Z_r. \quad (15)$$

Hence, it is now straightforward to calculate the stiffness and damping coefficients [16].

### Bearing Geometry and Computational Domain

The studied bearing geometry is from Dickman [17], which was designed and manufactured by NASA. The geometry and material properties of the tested thrust foil bearing can be found in Ref. [17, 1].

The computational domain for the foil thrust bearing simulation is shown in Fig. 2. As foil thrust bearings consist of six thrust pads, only one pad is simulated to reduce the computational cost. The top surface is the rotor while the bottom surface is the top foil. The rotational direction is shown in Fig. 2. Boundary conditions at the surrounding surfaces are modeled as fixed static pressure and temperature, and the top wall is regarded as a moving wall with constant temperature, the bottom (top foil) is set as the constant temperature wall and coupled with the structural deformation solver, allowing a deformed foil shape to be analysed.

### Verification

As mentioned in Ref. [3, 12], the structural deformation solver is executed at the comparatively large time step  $\Delta t_s$  during the fluid-structure simulation to obtain the steady state performance. To accurately predict the dynamic performance of foil thrust bearings,  $\Delta t_s$  has to be selected properly. This is discussed at the end of this section. The rotational speed of foil thrust bearings is set as 21 000 rpm, matching the operating conditions from the experiment [17]. San Andrés [1] investigated the rotordynamic performance of foil thrust bearings at the synchronous

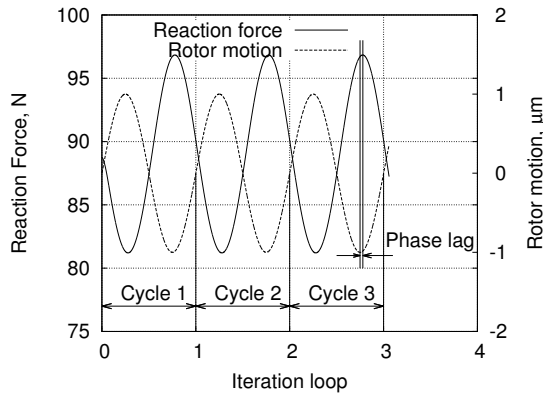


Figure 3: History plot of reaction force and rotor motion.

excitation frequency and the numerical results are used as the verification case.

The optimal mesh ( $48 \times 96 \times 15$ ) for foil thrust bearings has been attained previously [3] and is used in this paper. In order to establish time-step independence, the number of oscillations required to reach a steady response has to be determined. The time history of the reaction force and rotor motion for a time step of  $2 \mu\text{s}$  (for the structural deformation solver) is depicted in Fig. 3. The phase lag is labelled also. The magnitude is approximately  $10^3$  ( $80 \mu\text{s}$ ). The rotordynamic coefficients are then calculated from the different cycles and compared in Fig. 4. It is found that the results converge after two periods. This matches the observations from Ref. [16].

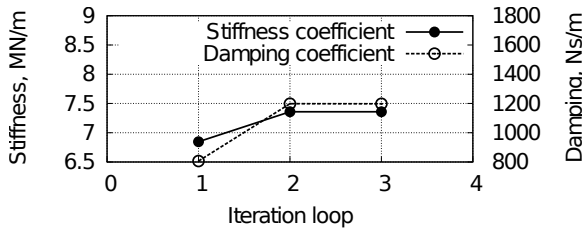


Figure 4: Comparison of the calculated stiffness and damping coefficient at different iteration loop.

Three different time steps  $\Delta t_s$  ( $2 \mu\text{s}$ ,  $1 \mu\text{s}$  and  $0.5 \mu\text{s}$ ) are used to compare the numerical results for the fluid-structure simulations. The results are shown in Fig. 5(a) and are all calculated during the second harmonic motion of the rotor. Insensitivity to the size of the time step is observed and  $1 \mu\text{s}$  is selected in the subsequent analysis. The perturbation amplitude (5%, 10% and 15% of the clearance) is compared in Fig. 5(b). This indicates the insensitivity of results to excitation amplitude. A 10% perturbation amplitude is used for following studies.

San Andrés et. al. [1] predicted the synchronous rotordynamic performance of air foil thrust bearings at the rotational speed of 21000rpm. This method is based on the small perturbation of Reynolds equation and used as the verification case. The comparison results are compared in Fig. 6. Good agreement is achieved at the various load conditions for damping coefficients. A slight difference is found for stiffness coefficients, this can be attributed to different models used. However, the trend in terms of load capacity is the same.

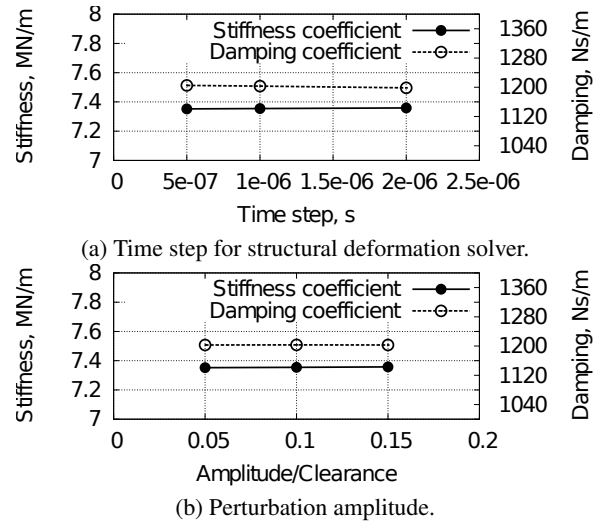


Figure 5: Comparison of the calculated stiffness and damping coefficient at different parameters.

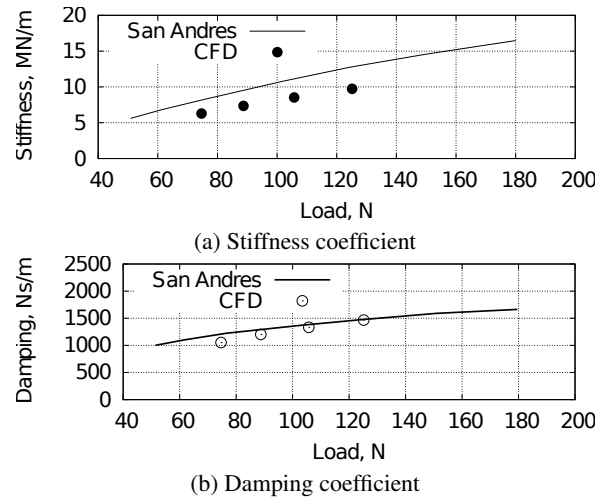


Figure 6: Comparison of CFD and numerical results from San Andrés [1], rotational speed: 21000rpm.

### Dynamic Performance of CO<sub>2</sub> Foil Thrust Bearings

In this section, the numerical simulations are conducted by replacing air with CO<sub>2</sub> and the rotational speed is maintained at 21000rpm. The operating pressure and temperature are 1.4MPa and 300K, respectively. The synchronous rotordynamic coefficients at various load conditions were obtained and shown in Fig. 7. For CO<sub>2</sub> foil thrust bearings, the stiffness coefficient is close to that for air. However, a significant difference is observed for the damping coefficient. The damping coefficients is around 200Ns/m, which is less than 20% of the value for air foil bearings. The phase lag for CO<sub>2</sub> foil thrust bearings is  $1^\circ$  at the rotational speed of 21000rpm. This can be attributed to inertia effect and much higher Reynolds numbers leading to turbulent flow in the sCO<sub>2</sub> foil bearing. Typically inertia effects tend to reduce damping coefficients, while turbulence effects can augment damping. These two effects play the opposite role for the rotordynamic performance of foil thrust bearings [18, 19]. A more detailed analysis has to be conducted to further investigate the dynamic performance of CO<sub>2</sub> foil thrust bearings.

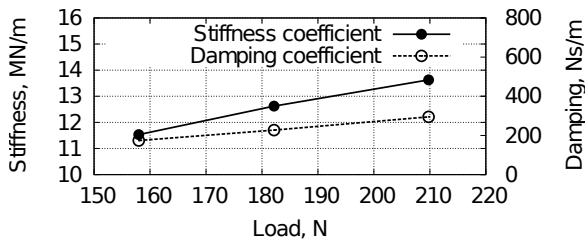


Figure 7: Calculated synchronous stiffness and damping coefficients for CO<sub>2</sub> foil thrust bearings, rotational speed: 21 000 rpm.

### Conclusions and Future Work

In this paper, the dynamic performance of foil thrust bearings is investigated with CFD. The method to extract stiffness and damping coefficients are detailed and verified with the results from the literature. It is found that transient CFD approach can be used to predict the dynamic performance of foil thrust bearings and that CO<sub>2</sub> foil thrust bearings experience reduced damping effects due to different phase lag. So far, the work has been verified through comparison to numerical results from literature and good agreement has been observed.

### Acknowledgements

This research was performed as part of the Australian Solar Thermal Research Initiative (ASTRI), a project supported by Australian Government. The first author, Kan Qin, would also like to thank China Scholarship Council and The University of Queensland and Queensland Geothermal Energy Centre of Excellence for their financial support. This work was supported by resources provided by The Pawsey Supercomputing Centre with funding from the Australian Government and the Government of Western Australia.

### References

[1] San Andrés, L.A. and Diemer, P., Prediction of gas thrust foil bearing performance for oil-free automotive turbochargers, *ASME Journal of Engineering for Gas Turbines and Power*, **137**(3), 2014, 032502.

[2] Wright, S.A. and Radell, P.A., Vernon, M.E. and Rochau, G.E. and Pichard, P.S., Operation and analysis of a Supercritical CO<sub>2</sub> Brayton cycle, *Sandia National Laboratories, SAN2010-0171*, 2010.

[3] Qin, K. and Jahn, I.H. and Jacobs, P.A., Development of a computational tool to simulate foil bearings for supercritical CO<sub>2</sub> cycles, *ASME Journal of Engineering for Gas Turbines and Power*, **138**, 2016, 092503.

[4] Qin, K. and Jahn, I.H. and Jacobs, P.A., Effect of operating conditions on the elasto-hydrodynamic performance of foil thrust bearings for supercritical CO<sub>2</sub> cycles, *ASME Turbo Expo 2016: Turbomachinery Technical Conference and Exposition*, Seoul, South Korea, 13-17 June, 2016.

[5] Li, Z. and Li, J. and Feng, Z., Comparisons of rotordynamic characteristics predictions for annular gas seals using the transient computational fluid dynamic method based on different single-frequency and multifrequency rotor whirling models, *ASME Journal of Tribology*, **138**, 2016, 011701.

[6] Papadopoulos, C.I. and Nikolakopoulos, P.G. and Kaiktsis, L., Characterization of stiffness and damping in textured sector pad micro thrust bearings using computational fluid

dynamics, *ASME Journal of Engineering for Gas Turbines and Power*, **134**, 2012, 112502.

[7] Park, D.J. and Kim, C.H. and Jang, G.H., Theoretical considerations of static and dynamic characteristics of air foil thrust bearing with tilt and slip flow, *Tribology International*, **41**, 2008, 282-295.

[8] Jacobs, P.A. and Gollan, R.J. and Jahn, I. and Potter D.F., The Eilmer3 code: user guide and example book 2015 edition, *Mechanical Engineering Report, The University of Queensland*, **2015/07**, 2015.

[9] Gollan, R.J. and Jacobs, P.A., About the formulation, verification and validation of the hypersonic flow solver Eilmer, *International Journal for Numerical Methods in Fluids*, **73**, 2013, 19-57.

[10] Qin, K. and Jahn, I.H. and Jacobs, P.A., Validation of a three-dimensional CFD analysis of foil bearings with Supercritical CO<sub>2</sub>, *The 19th Australasian Fluid Mechanics Conference*, Melbourne, Australia, 8-11 December, 2014.

[11] Qin, K. and Jahn, I.H., Structural deformation of a circular thin plate with combinations of fixed and free edges, *Mechanical Engineering Report, The University of Queensland*, **2015/05**, 2015.

[12] Qin, K. and Jahn, I.H. and Jacobs, P.A., Development of a fluid-structure Model for gas-lubricated bump-type foil thrust bearings, *The 2nd Australasian Conference on Computational Mechanics*, Brisbane, Australia, November to December, 2015.

[13] Lemmon, E.W. and Huber, M.L. and McLinden, M.O., NIST standard reference database 23: reference fluid thermodynamic and transport properties-REFPROP, Version 9.1, *National Institute of Standards and Technology, Standard Reference Data Program*, Gaithersburg, 2013.

[14] Span, R. and Wagner, W., A new equation of state for carbon dioxide covering the fluid region from triple-point temperature to 1100 K at pressures up to 800 MPa, *Journal of Physical and Chemical Reference Data*, **25**(6), 1996, 1509-1596.

[15] Childs, D. editor *Turbomachinery rotordynamics: phenomena, modelling, and analysis* Hoboken, New Jersey, John Wiley Sons, Inc., 1997.

[16] Yan, X. and He, K. and Li, J. and Feng, Z.P., A generalized prediction method for rotordynamic coefficients of annular gas seals, *ASME Journal of Engineering for gas turbines and power*, **137**, 2015, 092506.

[17] Dickman, J.R., An investigation of gas foil thrust bearing performance and its influence factors, Master thesis, Case Western Reserve University, 2015.

[18] Nataraj, C. and Ashrafiuon, H. and Arakere, N., Effect of fluid inertia on journal bearing parameters, *Tribology Transactions*, **37**, 1994, 784-792.

[19] Dousti, S. and Cao, J. and Younan, A. and Allaire, P. and Dimond, T., Temporal and convective inertia effects in plain journal bearings with eccentricity, velocity and acceleration, *ASME Journal of Tribology*, **134**, 2012, 031704.